

AD-A058 600

NAVAL RESEARCH LAB WASHINGTON D C
PERFORMANCE OF AN ANTENNA SHARING THE APERTURE OF A FREQUENCY-S--ETC(U)
MAY 78 R M BROWN

F/G 9/5

UNCLASSIFIED

NRL-8226

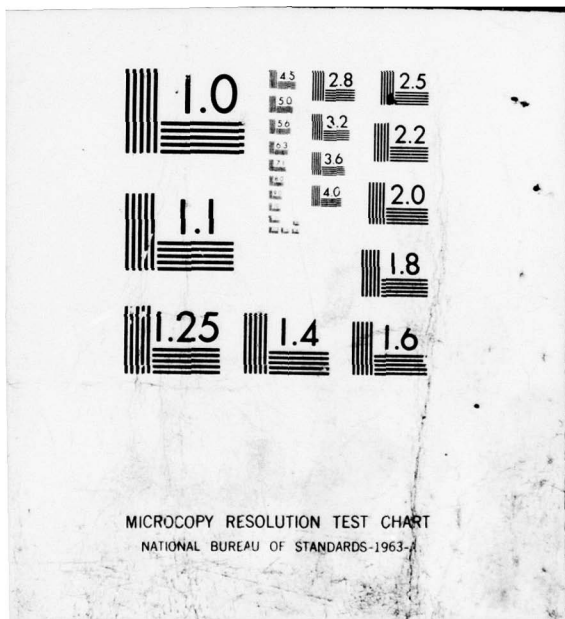
SBIE-AD-E000 194

NL

| OF |
AD
A058 600



END
DATE
FILED
11-78
DDC



AD A0 58600

AD No. _____
DDC FILE COPY

(13) NW
LEVEL II

ade 000194
NRL Report 8226

Performance of an Antenna Sharing the Aperture of a Frequency-Scanned Array

RUSSELL M. BROWN

*Target Characteristics Branch
Radar Division*

May 12, 1978

78 08 01 006



NAVAL RESEARCH LABORATORY
Washington, D.C.

Approved for public release; distribution unlimited.

(18) SBIE

(19) AD-E660 194

UNCLASSIFIED

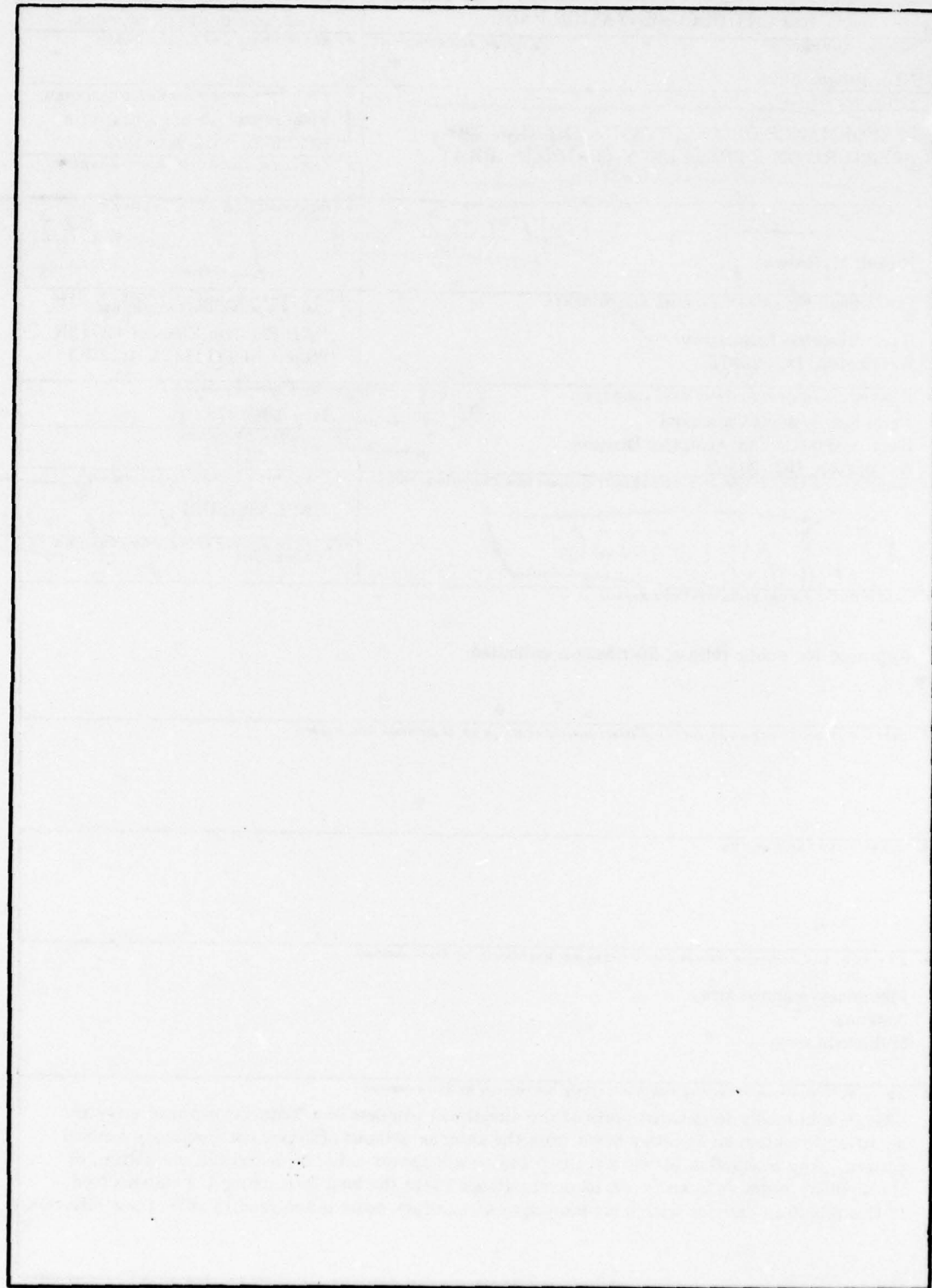
SECURITY CLASSIFICATION OF THIS PAGE (When Data Entered)

REPORT DOCUMENTATION PAGE		READ INSTRUCTIONS BEFORE COMPLETING FORM
1. REPORT NUMBER NRL Report 8226	2. GOVT ACCESSION NO.	3. RECIPIENT'S CATALOG NUMBER
4. TITLE (and Subtitle) PERFORMANCE OF AN ANTENNA SHARING THE APERTURE OF A FREQUENCY-SCANNED ARRAY.		5. TYPE OF REPORT & PERIOD COVERED Final report, in one phase of a continuing NRL problem.
6. AUTHOR(s) Russell M. Brown	16 F12141	7. PERFORMING ORGANIZATION NAME AND ADDRESS Naval Research Laboratory Washington, DC 20375
8. CONTRACTOR OR GRANT NUMBER(s) SF12141491		9. PROGRAM ELEMENT, PROJECT, TASK AREA & WORK UNIT NUMBERS NRL Problem Element 62712N Project SF12141491 R12-53
10. CONTROLLING OFFICE NAME AND ADDRESS Naval Sea Systems Command Electromagnetic and Acoustics Division Washington, DC 20362		11. REPORT DATE May 1978
12. MONITORING AGENCY NAME & ADDRESS (if different from Controlling Office) 14 NRL-8226		13. NUMBER OF PAGES 22
14. DISTRIBUTION STATEMENT (of this Report) Approved for public release; distribution unlimited		
15. SECURITY CLASS. (of this report) UNCLASSIFIED		
15a. DECLASSIFICATION/DOWNGRADING SCHEDULE 12/22 p.m.		
16. DISTRIBUTION STATEMENT (of the abstract entered in Block 20, if different from Report)		
17. SUPPLEMENTARY NOTES		
18. KEY WORDS (Continue on reverse side if necessary and identify by block number) Frequency-scanned array Antenna Multibeam array		
19. ABSTRACT (Continue on reverse side if necessary and identify by block number) The normally terminated ports of the directional couplers in a frequency-scanned array can be driven to obtain an auxiliary beam from the antenna without affecting the frequency-scanned pattern. Any interaction between the two beams will appear either as changes in the pattern of the auxiliary beam or in an excess of power dumped into the load terminating the sinuous feed. In this report an antenna with a cosecant-squared auxiliary beam is analyzed to show these effects.		

251 950 78 08 01 006 *Gu*

UNCLASSIFIED

SECURITY CLASSIFICATION OF THIS PAGE (When Data Entered)



UNCLASSIFIED

SECURITY CLASSIFICATION OF THIS PAGE (When Data Entered)

CONTENTS

INTRODUCTION	1
GENERAL ANALYSIS	2
EXAMPLE: COSECANT-SQUARED AUXILIARY BEAM	3
SUMMARY	12
APPENDIX A - Distribution of Coupling Coefficients	13
APPENDIX B - Synthesis of a Csc ² Pattern	14
APPENDIX C - Network Formulation for Power Dumped	16
APPENDIX D - Patterns for Single-Port Excitation	18

ACCESSION for		
NTIS	White Section <input checked="" type="checkbox"/>	
DDC	Buff Section <input type="checkbox"/>	
UNANNOUNCED <input type="checkbox"/>		
JUSTIFICATION _____		
BY _____		
DISTRIBUTION/AVAILABILITY CODES		
Dist. AVAIL and/or SPECIAL		
A		

PERFORMANCE OF AN ANTENNA SHARING THE APERTURE OF A FREQUENCY-SCANNED ARRAY

INTRODUCTION

Many frequency-scanned arrays can be modified so that all or part of the aperture can be used as an auxiliary antenna operating simultaneously with the frequency-scanned system. Such antennas use directional couplers to couple energy from the sinuous (serpentine) transmission line to the radiating elements. Each coupler has a port normally terminated but into which a signal may be introduced to excite part of the antenna. Any number of these terminals may be fed as an array, as in Fig. 1, to achieve particular pattern shapes and, because of the isolation provided by the couplers, have essentially no effect on the frequency-scanned beam. Shelton of this Laboratory suggested* that this technique be considered for adding a fan beam to existing frequency-scanned arrays to provide a 2D search beam with the frequency diversity not possible with a frequency-scanned pencil beam. Unknown to Shelton, Ajioka had recognized some years earlier† that these normally terminated ports provided free access to the radiators and had demonstrated that two separate elements could be used in this way for an auxiliary sidelobe-suppression antenna.

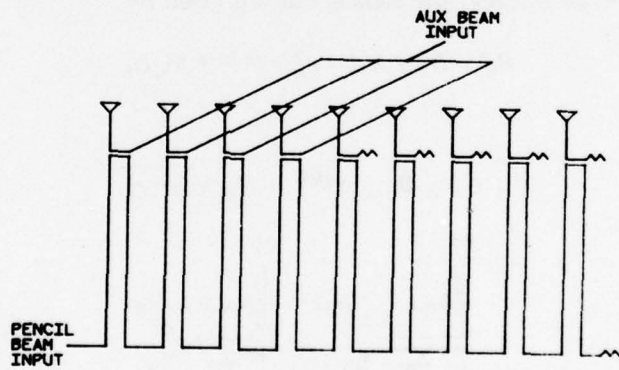


Fig. 1 — Schematic diagram of the normally terminated ports of a frequency-scanned array used for an auxiliary beam

Although the frequency-scanned beam is not affected by the use of the terminated ports (assuming that reasonable match is maintained), some kind of interaction is to be expected when a single aperture is used to form two separate beams; hence a disturbance is likely in the pattern of the auxiliary antenna at the angle in which the frequency-scanned beam is pointed, and an excessive amount of the auxiliary-beam power might

*J.P. Shelton, "Combined Fan-Beam and Frequency-Scanned Pencil-Beam Antenna," memorandum, Mar. 1975, unpublished.

†J.S. Ajioka, "Integral Auxiliary Antennas Derived from Arrays of Directionally Coupled Elements," invention disclosure, Feb. 1962, unpublished.

be dumped into the load terminating the sinuous line. This report considers the configuration suggested by Shelton, a frequency-scanned pencil-beam array with an auxiliary cosecant-squared antenna, but the results for this specific problem indicate how other such antennas should be designed and what performance degradation might be expected.

GENERAL ANALYSIS

Before considering an example, some necessary relations will be developed. An idealized system is assumed: lossless, matched, and dispersionless, with perfect directional couplers. For the couplers the convention to be followed is that the straight-through arm has phase 0 and the coupled (adjacent) arm leads in phase by 90 degrees; With unit signal incident at any port of the coupler, the signal from the direct port is $\sqrt{1 - c^2}$, from the coupled port jc , and from the isolated port 0.

Figure 2 shows successive elements of the array connected by a length L of transmission line. The relationships among the currents incident on and scattered from a given coupler are used in determining the proper input currents for the auxiliary beam and then in finding the current distribution on the array for a given auxiliary-beam excitation and frequency. As indicated in the figure, c_n is the voltage-coupling coefficient of the n th coupler, A_n the signal incident on the radiating element, B_n the signal leaving the coupler on the sinuous line, and D_n the signal into the port normally terminated and which is to be used for the auxiliary beam. A_n , B_n , and D_n are complex, and c_n is real and positive. The signal on the sinuous line incident on the n th coupler is $B_{n-1} e^{jkL}$, with $k = 2\pi / \lambda$, and the signals out are given by

$$B_n = B_{n-1} \sqrt{1 - c_n^2} e^{-jkL} + jc_n D_n \quad (1)$$

and

$$A_n = jc_n B_{n-1} e^{-jkL} + D_n \sqrt{1 - c_n^2}. \quad (2)$$

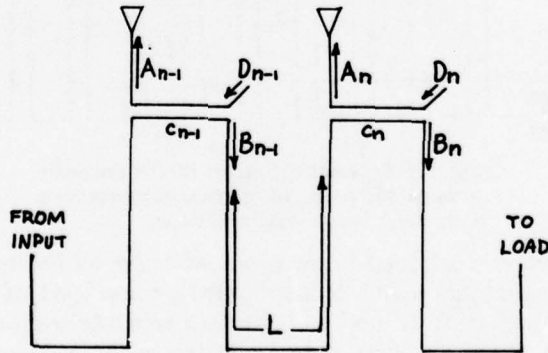


Fig. 2 — Currents on adjacent couplers of the sinuous feed

First, the auxiliary-beam inputs D_n are determined for a given distribution of coupling coefficients and specified currents A_n on the radiating elements. If the elements to be used for the auxiliary beam are the p th through the $(p + q)$ th, the inputs, normalized to the first input D_p , are found sequentially in the following way. At the first coupler used, no signal is incident via the sinuous line, so from (1) and (2) the signals to the next coupler and to the radiating element are

$$B_p = jc_p D_p \text{ and } A_p = D_p \sqrt{1 - c_p^2}. \quad (3)$$

At the second coupler, the element current A_{p+1} is given (relative to A_p) and the signal incident via the sinuous feed is known, so the necessary auxiliary-beam input is found from (2) as

$$D_{p+1} = (A_{p+1} - jc_{p+1} B_p e^{jkL}) / \sqrt{1 - c_p^2} \quad (4)$$

and the signal on the serpentine B_{p+1} is found from (1). This procedure is repeated element by element until all the $q + 1$ auxiliary-beam input currents have been determined. At the frequency at which they are calculated, these input currents produce precisely the currents specified on the $q + 1$ elements, but at another frequency the electrical length of the feed-line loops is different, so the element currents and therefore the radiation pattern must change. Moreover, at all frequencies, all elements following the $(p + q)$ th will be excited by the signal left on the sinuous line. Since the element currents change with frequency, it is not evident a priori that the fan-beam input currents could not as well be determined solely from the coupling coefficients, neglecting currents on the serpentine, that is, using $D_n = A_n / \sqrt{1 - c_n^2}$ for all the $q + 1$ elements.

After the input currents have been determined, the performance of the auxiliary antenna is evaluated as a function of frequency by finding the currents on all elements from the p th onward (from (1) and (2)) and then using these to calculate the radiation pattern, directivity, and power dumped.

EXAMPLE: COSECANT-SQUARED AUXILIARY BEAM

The parameters of the frequency-scanned array used in the example that follows were chosen to be similar to those of an antenna of practical dimensions which might be used for a height-finding radar. Most such antennas are planar, scanned by frequency in elevation and by mechanical rotation in azimuth, so the patterns to be shown correspond to elevation-plane patterns; directivity will be only relative, since it is based on the integration of the elevation pattern alone. The array consists of 61 elements with a 6-wavelength length of line between the elements (at the broadside frequency), so that the beam scans about 35 degrees for a 5-percent change in frequency. The coupling coefficients are determined (Appendix A) from the amplitude distribution that is specified for the array and by the power that is to be dumped in the load (the distribution used was cosine on a pedestal of 0.1, with 3 percent of the power dumped). The resulting distribution of coupling coefficients (Fig. 3) shows coupling values ranging from about 27 to 9 dB.

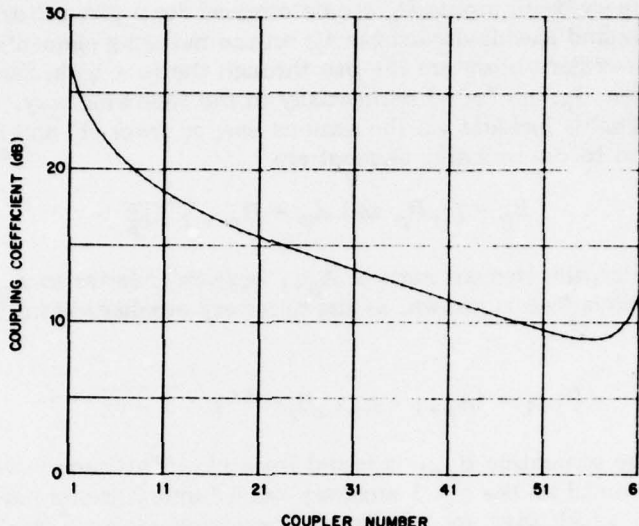


Fig. 3 — Coupling coefficients for a 61- element sinuous feed

The auxiliary beam is to use 18 of the elements, which could be anywhere along the 61-element array, but only the two extreme positions will be considered: elements 1 through 18, where the couplers are weakest, and elements 44 through 61, where they are strongest. What would result for other positions on the array can be deduced from these cases. The array broadside direction is horizontal (0 degrees), and the auxiliary beam is to have approximately a cosecant-squared shape to 35 degrees in elevation. A current distribution appropriate to the \csc^2 pattern, obtained from a Woodward synthesis (Appendix B), is shown in the columns of Table 1 labeled V ANT, and the resultant pattern for $\lambda/2$ spacing is shown in Fig. 4.

First, elements 1 through 18 are used. The one parameter left is the wavelength λ_0 at which the shaped-beam input currents are calculated. Two values of λ_0 will be used: one for which the frequency-scanned beam coincides with the main part of the shaped pattern, and one for which it does not. The two are $\lambda_0 = 1.01$, for which the pencil beam points about 7 degrees above the horizon, nearly at the peak of the \csc^2 pattern, and $\lambda_0 = 0.95$, for which the pencil beam points about 37 degrees down, well into the side-lobe region of the \csc^2 pattern. The input currents for these wavelengths are in Table 1, in the columns labeled V IN. Table 1 indicates that for $\lambda_0 = 0.95$ the input currents are nearly identical to the specified element currents, this due to the weak coupling (16 to 27 dB) at the first 18 elements and to the lack of any resonant buildup of current on the sinuous line. For $\lambda_0 = 1.01$ the input currents at the later elements are forced by currents on the sinuous line to differ more from the element currents.

Next the performance of the auxiliary antenna was calculated for a number of frequencies by finding all 61 element currents with the 18 input currents held fixed and, from these currents, finding the pattern and directivity. Patterns for $\lambda = 0.98, 1.01, 1.03$,

NRL REPORT 8226

Table 1 - Auxiliary-beam input excitations (AMP = amplitude and PH D = phase in degrees) to achieve the specified element excitations (elements 1 through 18 driven; design wavelength $\lambda_0 = 1.01$ and 0.95)

N	V ANT		V IN (1.01)		V IN (.95)	
	AMP	PH D	AMP	PH D	AMP	PH D
1	0.343	- 2.92	0.343	- 2.92	0.343	- 2.92
2	0.369	- 46.91	0.390	- 46.78	0.390	- 47.04
3	0.677	- 45.38	0.681	- 45.24	0.677	- 45.49
4	0.716	- 46.43	0.722	- 46.15	0.716	- 46.50
5	1.045	- 56.06	1.054	- 55.62	1.047	- 56.17
6	1.380	- 43.94	1.398	- 43.49	1.381	- 44.08
7	1.453	- 43.89	1.479	- 43.11	1.454	- 44.04
8	2.287	- 43.79	2.324	- 42.98	2.292	- 43.93
9	3.293	- 17.13	3.367	- 16.62	3.294	- 17.25
10	3.293	17.13	3.418	17.27	3.291	17.03
11	2.287	43.79	2.456	43.67	2.284	43.57
12	1.453	43.89	1.651	46.20	1.451	43.55
13	1.380	43.94	1.577	49.20	1.380	43.74
14	1.045	56.06	1.252	64.50	1.043	55.68
15	0.718	46.43	0.851	65.22	0.714	45.93
16	0.677	45.38	0.735	68.78	0.677	45.19
17	0.369	46.91	0.411	83.27	0.366	46.20
18	0.343	2.92	0.040	61.22	0.344	2.01

V ANT-----SPECIFIED ELEMENT EXCITATIONS

V IN (X)--AUX BEAM INPUTS FOR WAVELENGTH X

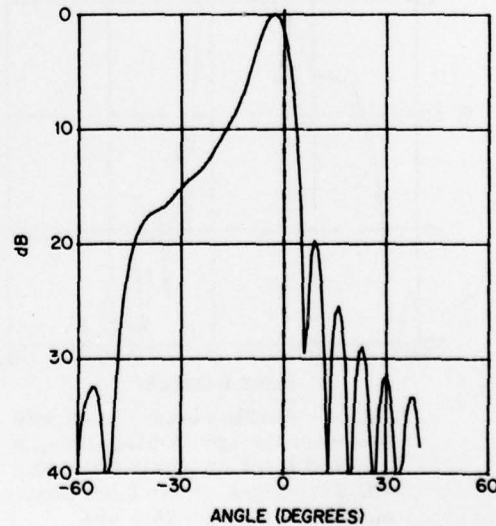


Fig. 4 - Synthesized cosecant-squared pattern (18 elements; seven-mode synthesis as shown in Fig. B1). Negative angles are above the horizon.

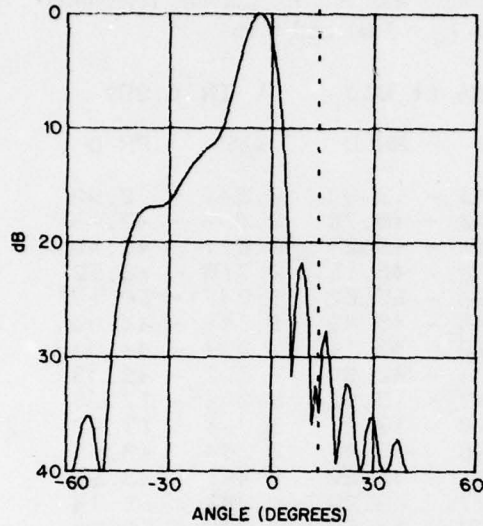


Fig. 5a - Auxiliary-beam pattern with elements 1 through 18 driven for $\lambda_0 = 1.01$ and $\lambda = 0.98$ (directivity = 15.1 dB, 0.0 percent of the input power dumped, and gain = 15.1 dB)

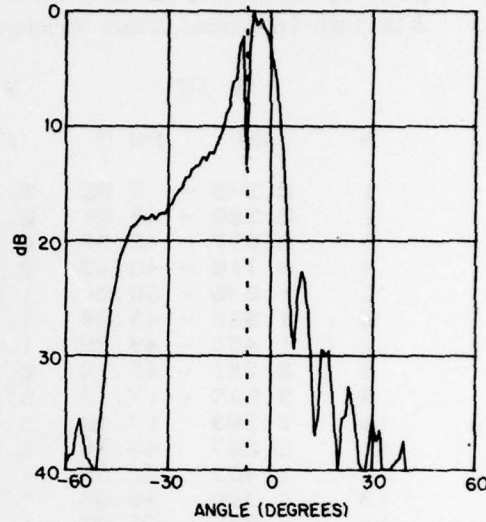


Fig. 5b - Auxiliary-beam pattern with elements 1 through 18 driven for $\lambda_0 = 1.01$ and $\lambda = 1.01$ (directivity = 15.3 dB, 0.3 percent of the input power dumped, and gain = 15.3 dB)

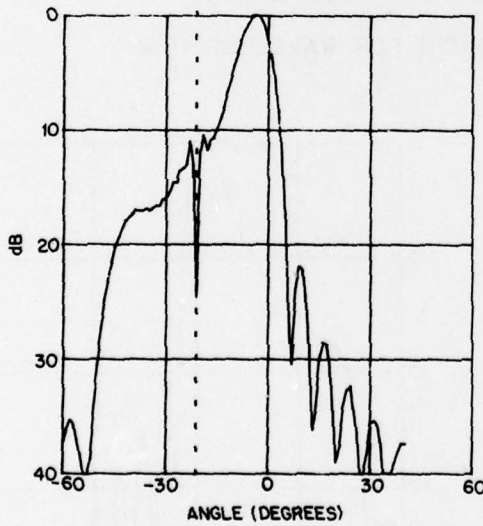


Fig. 5c - Auxiliary-beam pattern with elements 1 through 18 driven for $\lambda_0 = 1.01$ and $\lambda = 1.03$ (directivity = 15.3 dB, 0.0 percent of the input power dumped, and gain = 15.3 dB)

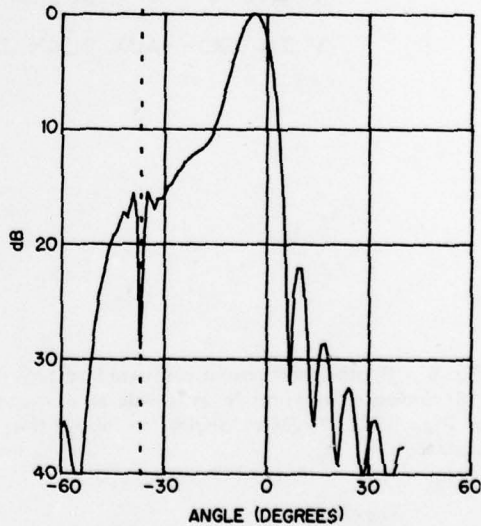


Fig. 5d - Auxiliary-beam pattern with elements 1 through 18 driven for $\lambda_0 = 1.01$ and $\lambda = 1.05$ (directivity = 15.0 dB, 0.0 percent of the input power dumped, and gain = 15.0 dB)

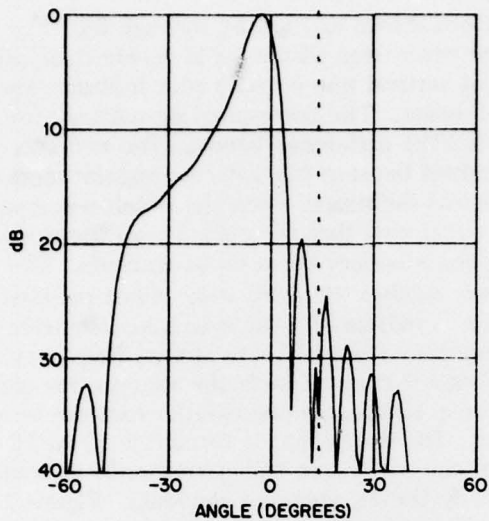


Fig. 6a - Auxiliary-beam pattern with elements 1 through 18 driven for $\lambda_0 = 0.95$ and $\lambda = 0.98$ (directivity = 15.2 dB, 0.0 percent of the input power dumped, and gain = 15.2 dB)

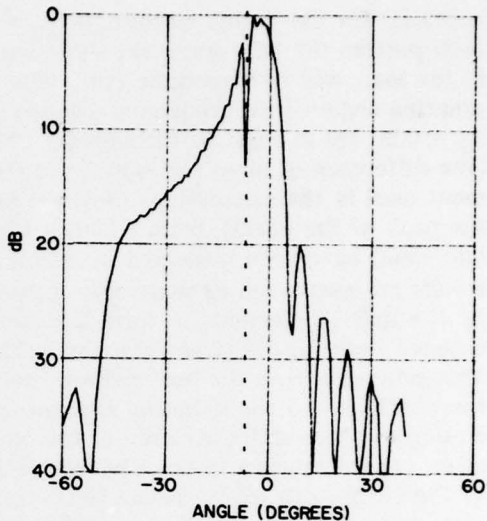


Fig. 6b - Auxiliary-beam pattern with elements 1 through 18 driven for $\lambda_0 = 0.95$ and $\lambda = 1.01$ (directivity = 15.6 dB, 0.3 percent of the input power dumped, and gain = 15.6 dB)

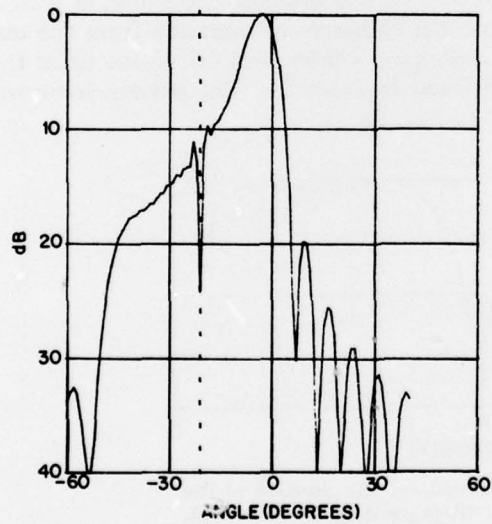


Fig. 6c - Auxiliary-beam pattern with elements 1 through 18 driven for $\lambda_0 = 0.95$, and $\lambda = 1.03$ (directivity = 15.0 dB, 0.0 percent of the input power dumped, and gain = 15.0 dB)

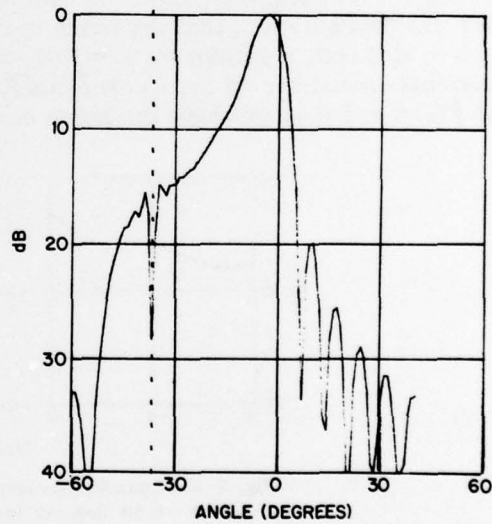


Fig. 6d - Auxiliary-beam pattern with elements 1 through 18 driven for $\lambda_0 = 0.95$ and $\lambda = 1.05$ (directivity = 14.9 dB, 0.0 percent of the input power dumped, and gain = 14.9 dB)

R.M. BROWN

and 1.05 for the design wavelength $\lambda_0 = 1.01$ are shown as Figs. 5a through 5d. For each pattern the title states the directivity, the percentage of the input power dissipated in the load, and the resultant gain. The dashed vertical line on each plot indicates the pointing angle of the frequency-scanned pencil beam. The corresponding patterns for $\lambda_0 = 0.95$ are in Figs 6a through 6d. There is little difference between the two sets (the difference in directivities at $\lambda = 1.01$ occurred because the 1-degree angular increment used in the calculations provided insufficient definition when the notch was near the peak of the beam), from which it can be concluded that the currents on the sinuous line could have been neglected in determining the auxiliary-beam input currents. The results are nearly self-explanatory. Little power reaches the load; what is not radiated by the first 18 elements to form the csc^2 beam is radiated by the remaining elements as a pencil beam in the same direction as the frequency-scanned beam at that frequency. This subtracts from the csc^2 pattern, because signals coupled onto the sinuous line and then back out to the radiating elements acquire a 180-degree phase shift from the two 90-degree phase shifts incurred at the couplers. The notch that is formed is 10 to 15 dB deep when it appears in the coverage region of the csc^2 beam and corresponds in width to the beamwidth of the pencil beam radiated by the 43 undriven elements. Figure 7 is an expanded pattern of the notch shown in Fig. 6b. At wavelengths for which the frequency-scanned beam is pointed into the sidelobe region of the csc^2 beam (as for example in Fig. 6a), the lobe radiated by the undriven elements is at a low level because little power was left to be radiated. This is illustrated in Table 2, which shows the currents on the radiating elements and the current on the sinuous feed at each of the first 18 couplers for wavelengths of 0.98 and 1.01 (the corresponding patterns are in Figs. 6a and 6b). The resonant buildup on the line for $\lambda = 1.01$ is evident. To show, at least for this configuration, that the notch in the pattern comes from radiation from the undriven elements, a pattern for $\lambda = 1.01$, with design $\lambda_0 = 0.95$, was calculated using the currents on just the 18 driven elements (those listed in Table 2). The pattern is shown as Fig. 8 and does not have the notch evident in Fig. 6b.

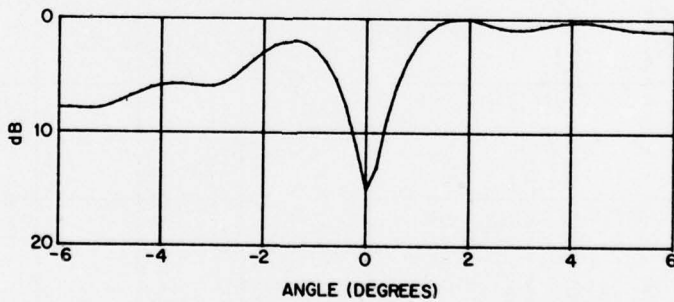
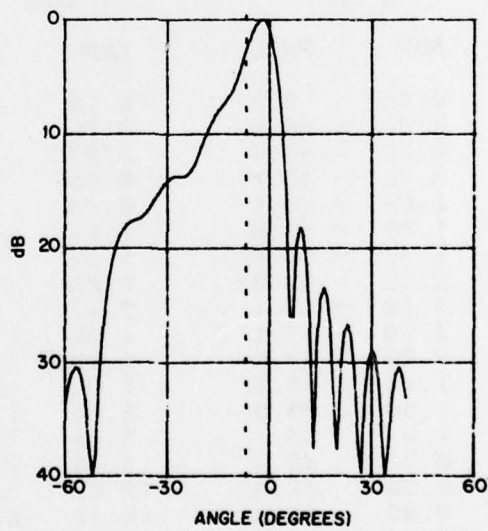


Fig. 7 - Expanded pattern centered on the position of the notch at -6.89 degrees in Fig. 6b ($\lambda_0 = 0.95$, $\lambda = 1.01$ and, elements 1 through 18 driven)

NRL REPORT 8226

Table 2 - Currents on the driven elements (V ANT) and currents on the sinuous feed (V SERP OUT) with $\lambda_0 = 0.95$ and elements 1 through 18 driven

WAVELENGTH=.98				WAVELENGTH=1.01				
N	V ANT AMP	V ANT PH D	V SERP OUT AMP	V SERP OUT PH D	V ANT AMP	V ANT PH D	V SERP OUT AMP	V SERP OUT PH D
1	0.34	- 2.9	0.02	87.1	0.34	- 2.9	0.02	87.1
2	0.39	- 47.0	0.04	43.0	0.39	- 47.2	0.03	69.5
3	0.67	- 45.3	0.06	23.7	0.67	- 45.6	0.07	63.7
4	0.71	- 46.1	0.11	5.2	0.71	- 46.8	0.12	67.3
5	1.04	- 55.7	0.16	- 7.8	1.04	- 56.6	0.16	65.7
6	1.36	- 43.5	0.19	- 11.3	1.36	- 44.5	0.29	70.5
7	1.45	- 43.3	0.21	- 14.8	1.43	- 44.8	0.39	77.2
8	2.29	- 43.4	0.27	- 2.3	2.26	- 44.7	0.57	79.4
9	3.29	- 18.6	0.33	26.4	3.22	- 17.6	0.69	90.0
10	3.29	17.6	0.33	52.5	3.17	16.9	1.26	110.1
11	2.29	44.4	0.28	61.4	2.12	43.7	1.52	131.6
12	1.45	44.8	0.25	56.7	1.26	40.7	1.66	151.2
13	1.39	44.9	0.22	56.2	1.21	37.3	1.61	169.0
14	1.05	56.8	0.16	51.7	0.88	44.4	1.90	187.4
15	0.72	47.3	0.12	46.7	0.68	24.1	1.91	206.0
16	0.68	46.3	0.09	54.3	0.73	23.2	1.69	224.4
17	0.39	47.6	0.07	49.8	0.55	17.2	1.85	244.1
18	0.34	3.9	0.09	40.5	0.62	- 1.0	1.77	265.3

Fig. 8 - Pattern of the auxiliary beam calculated from the currents on only the 18 driven elements (currents on elements 19 through 61 set equal to 0) with $\lambda_0 = 0.95$ and $\lambda = 1.01$

R.M. BROWN

In the second configuration the final 18 elements were used for the csc^2 beam. There were no undriven elements so any pattern distortion must come from the driven ones, unlike the first case. The couplers at the load end of the array are relatively strong (about 10 dB), so that much more energy is present on the sinuous feed either to distort the pattern or to be dumped. At the design wavelength the specified currents on the driven elements are always exactly realized. Since there are now no undriven elements, this must result in a notch-free pattern at the design wavelength, even through the frequency-scanned beam infringes on the shaped pattern. This is illustrated by Fig. 9a, the pattern for $\lambda = 1.01$ (with $\lambda_0 = 1.01$). The cost of the notch-free pattern is that 72 percent of the power is dumped. Table 3 shows the very large currents that are built up on the feed line in this case. With $\lambda = 1.03$ (still with $\lambda_0 = 1.01$) little power is dumped, but, as seen in Fig. 9b, the csc^2 coverage has been lost. Figures 10a and 10b show corresponding patterns for $\lambda_0 = 0.95$. For $\lambda = 1.01$ (Fig. 10a), 30 percent of the power is dumped, and there is a wide notch at the position of the frequency-scanned beam. For $\lambda = 1.03$ (Fig. 10b) a similar notch appears. For this configuration the notch width is commensurate with the pencil beam formed by 18 elements, since the out-of-phase beam which subtracts from the shaped beam comes from currents on just the driven elements. It is evident that the results were better when the weakly coupled elements were used.

Table 3 - Currents on the elements (V ANT) and on the sinuous feed (V SERP OUT) for $\lambda = 1.01$, $\lambda_0 = 1.01$, and elements 44 through 61 driven

N	V ANT		V SERP OUT	
	AMP	PH D	AMP	PH D
44	0.34	- 2.9	0.10	87.1
45	0.39	- 46.9	0.19	73.9
46	0.66	- 45.4	0.37	69.1
47	0.72	- 46.4	0.58	73.4
48	1.04	- 56.1	0.63	73.5
49	1.36	- 43.9	1.24	78.3
50	1.45	- 43.9	1.67	65.5
51	2.29	- 43.6	2.29	68.7
52	3.29	- 17.1	3.47	98.0
53	3.29	17.1	4.92	116.3
54	2.29	43.6	6.14	137.2
55	1.45	43.9	7.09	156.6
56	1.36	43.9	8.00	175.4
57	1.04	56.1	8.63	194.7
58	0.72	46.4	9.48	214.5
59	0.66	45.4	10.02	234.6
60	0.39	46.9	10.46	255.3
61	0.34	2.9	10.74	- 63.2

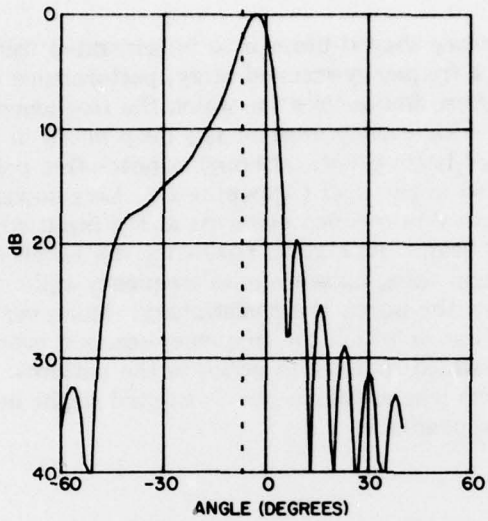


Fig. 9a - Auxiliary-beam pattern with elements 44 through 61 driven for $\lambda_0 = 1.01$ and $\lambda = 1.01$ (directivity = 15.0 dB, 72.0 percent of the input power dumped, and gain = 9.5 dB)

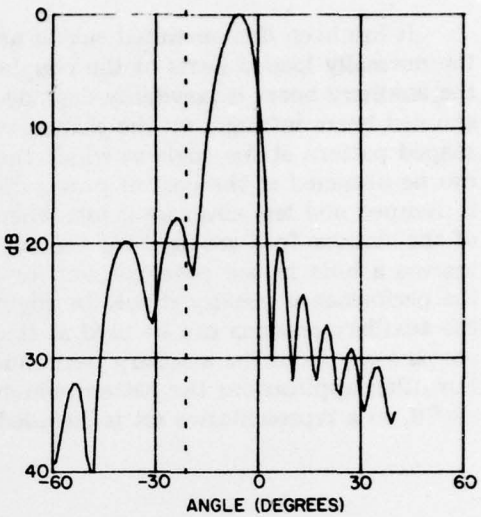


Fig. 9b - Auxiliary-beam pattern with elements 44 through 61 driven for $\lambda_0 = 1.01$ and $\lambda = 1.03$ (directivity = 15.7 dB, 1.2 percent of the input power dumped, and gain = 15.7 dB)

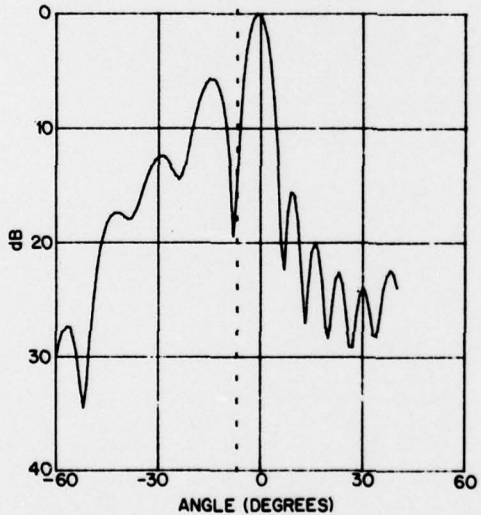


Fig. 10a - Auxiliary-beam pattern with elements 44 through 61 driven for $\lambda_0 = 0.95$ and $\lambda = 1.03$ (directivity = 15.6 dB, 29.7 percent of the input power dumped, and gain = 14.1 dB)

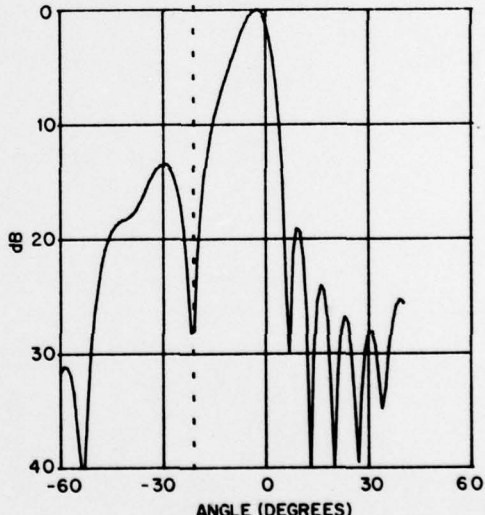


Fig. 10b - Auxiliary-beam pattern with elements 44 through 61 driven for $\lambda_0 = 0.95$ and $\lambda = 1.03$ (directivity = 15.0 dB, 3.0 percent of the input power dumped, and gain = 14.9 dB)

R.M. BROWN

SUMMARY

It has been demonstrated that if an auxiliary shaped beam is to be generated using the normally loaded ports of the couplers of a frequency-scanned array, performance of the auxiliary beam is inevitably degraded at those frequencies for which the frequency-scanned beam infringes on the shaped beam. This usually appears as a deep notch in the shaped pattern at the angle at which the pencil beam points, although a notch-free pattern can be obtained at the cost of power dissipated in the load (Appendix C). Less power is dumped and less coverage is lost when the weakly coupled elements at the input end of the sinuous feed are used for the auxiliary beam. At a given frequency the notch represents a hole in the coverage, but for a system using pulse-to-pulse frequency agility, the performance penalty should be slight, since the notch is not stationary. Moreover the auxiliary antenna can be used at frequencies for which the frequency-scanned beam points away from the auxiliary beam and for which there is no notch in the pattern. For other applications the pattern which results when a single port is excited might be useful, so a representative set is included in Appendix D.

Appendix A

DISTRIBUTION OF COUPLING COEFFICIENTS

One determines the coupling coefficients of the directional couplers on the sinuous line in sequence, knowing how much of the power incident on each coupler must be extracted to achieve a specified amplitude distribution on the array. Let c_n be the voltage coupling coefficient of the n th coupler, E_n the amplitude specified for the n th radiator, and F the fraction of the input power to be dumped in the load. The input power P_0 is then $(\sum E_n^2)/(1 - F)$. The power to be radiated by the first element is E_1^2 ; hence

$$c_1^2 = E_1^2/P_0.$$

The power incident on the second coupler is $P_0 - E_1^2$; hence

$$c_2^2 = E_2^2 / (P_0 - E_1^2).$$

This procedure is followed from element to element.

Appendix B

SYNTHESIS OF A CSC² PATTERN

A Woodward synthesis was used to find a current distribution producing an approximation to a csc^2 pattern. This is a power-pattern synthesis in which the aperture distribution is written as a sum of orthogonal modes whose amplitudes are adjusted so that the array pattern matches the desired pattern exactly at a discrete set of angles. Consider an N -element linear array with elements a distance S apart fed uniformly in amplitude with an interelement phase shift α . If θ is the angle from broadside, the radiation pattern is

$$E(\theta) = \frac{\sin(Nu/2)}{\sin(u/2)}, \quad u \equiv \frac{2\pi S}{\lambda} \sin \theta - \alpha. \quad (B1)$$

The set of distributions of this type with $\alpha = 0, 2\pi/N, 4\pi/N, \dots, (N-1)2\pi/N$ constitutes an orthogonal set of modes having pencil-beam patterns with peaks at θ_n satisfying $\sin \theta_n = 0, -2/N, -4/N, \dots, 4/N, 2/N$ respectively (for $\lambda/2$ spacing). These patterns have the property that at the angle of the peak of one mode pattern all other patterns have nulls, so a current distribution written as a sum of modes can be made to have a pattern matching a desired pattern at the angles θ_n by properly setting the relative amplitudes of the modes.

A realizable csc^2 pattern consists of a diffraction peak elevated about 1/2 beamwidth above the horizon with a tail that is attached to the upper side of the nose of the beam and that follows a csc^2 law to some specified elevation angle. A reasonable approximation is obtained as follows (Fig. B1). The diffraction nose is formed by feeding modes 0 and 1, which have peaks at $\sin \theta_0 = 0$ and $\sin \theta_1 = -2/N$, in phase with unit amplitudes. The resultant peak is at $\sin \theta = -1/N$ and is about 2 dB higher than the levels at θ_0 and θ_1 . The shaped tail results from setting the amplitudes of modes 2, 3, ... to match the csc^2 curve at $\theta_2, \theta_3, \dots$, with the csc^2 curve normalized to the angle of the upper 2-dB point at $\sin \theta_1 = -2/N$. Since the csc^2 curve is a power pattern, the amplitude of the m th mode is $csc \theta_m / csc \theta_1$, which equals $1/m$. For an 18-element array with coverage to about 35 degrees in elevation, it is necessary to use modes 0 through 6, since the peak of mode 5 is at 33 degrees elevation and the peak of mode 6 is at 42 degrees. Hence the synthesized current distribution is the result of summing modes 0 through 6, in phase, with amplitudes 1, 1, 1/2, 1/3, 1/4, 1/5, and 1/6 respectively.

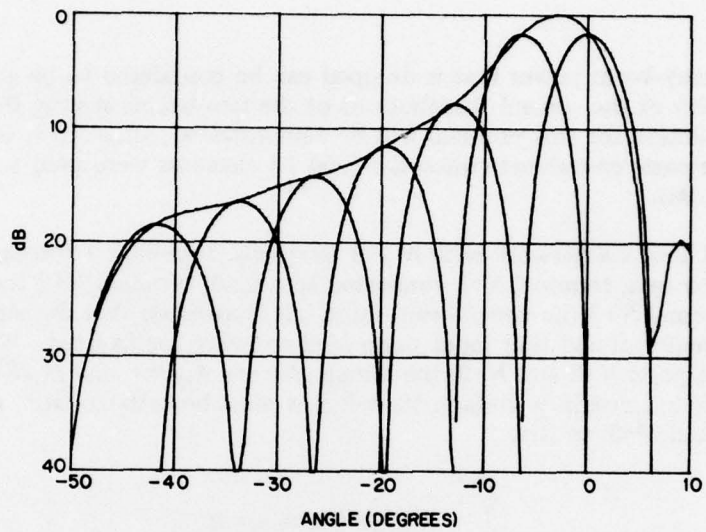


Fig. B1—Woodward synthesis of a \csc^2 pattern (seven modes being required to synthesize this pattern)

Appendix C

NETWORK FORMULATION FOR POWER DUMPED

The auxiliary-beam power that is dumped can be considered to be a result of the nonorthogonality of the current distributions of the two beams sharing the array. A network formulation for this problem will be demonstrated, although it is relevant to just one of the cases considered (when the final 18 elements were used to achieve the pattern in Fig. 9a).

Figure C1 shows a network with $N + 3$ terminals: terminals 1 through N connected to radiating elements, terminal $N+1$ connected to a load, terminal $N+2$ the auxiliary-beam input, and terminal $N+3$ the pencil-beam input. It is assumed that the network is matched, lossless, and reciprocal and that input ports $N+2$ and $N+3$ are isolated. When unit signals are incident on ports $N+2$ and $N+3$, the signals out are $A_n e^{j\alpha_n}$ and $B_n e^{j\beta_n}$ respectively. Since the scattering matrix is unitary, its columns must be orthogonal,* in particular columns $N+2$ and $N+3$, so that

$$\sum_{n=1}^{N+3} A_n B_n e^{j(\alpha_n - \beta_n)} = 0.$$

Since the input ports, $N+2$ and $N+3$, are matched and isolated, A_{n+2} , A_{n+3} , B_{n+2} , and B_{n+3} are zero, and we find that for the auxiliary beam the amplitude of the signal into the load is

$$B_{N+1} = \left| \sum_{n=1}^N A_n B_n e^{j(\alpha_n - \beta_n)} \right| / A_{N+1}, \quad (C1)$$

where A_{N+1} is the amplitude of the dumped pencil-beam signal.

As an example, a calculation was made using the parameters of the 61-element array with the 18-element \csc^2 beam. For the pencil beam, the element currents have amplitudes A_n , providing a cosine distribution on a pedestal of 0.1, and phases $\alpha_n = n\alpha$ for a linear phase progression over the array with pointing angle determined by the interelement phase shift α . Three percent of its power is to be dumped. The element currents $B_n e^{j\beta_n}$ for the auxiliary beam are the 18 currents shown in Table 1, and elements 44 through 61 are used. The percentage of the auxiliary-beam power dumped was calculated from (C1) as a function of the pointing angle of the pencil beam with the result

*G.G. Montgomery, R.H. Dicke, E.M. Purcell, editors *Principles of Microwave Circuits*, New York, McGraw-Hill, 1948, p. 149.

shown in Fig. C1. The basis for this curve is that the \csc^2 distribution remains fixed as the pencil beam is scanned; this was not the case for the frequency-scanned array, since then the distribution for the auxiliary beam changed as the beam was scanned. In the one applicable case, (Fig. 9a) 71 percent of the power was dumped when the wavelength was such that the pencil beam scanned to -7 degrees. This agrees with the loss curve in Fig. C1.

In general the loss curve depends on which elements are used for the auxiliary beam, but, because of the particular symmetry of the two current distributions used here, an identical curve results when elements 1 through 18 are used. This does not correspond to any case treated earlier, since then the elements following the 18th did not have zero current. This could have been achieved only by driving all 61 ports, not just the first 18.

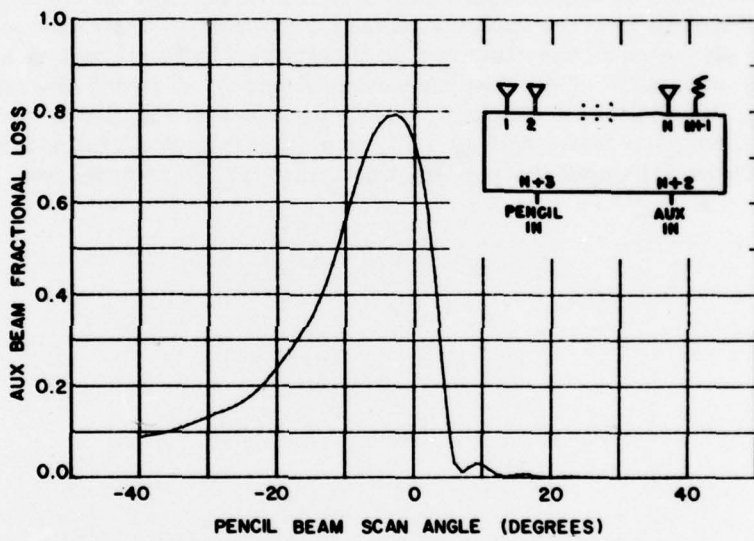


Fig. C1 — Power dumped when the \csc^2 beam and the scanning pencil beam use a common aperture

Appendix D

PATTERNS FOR SINGLE-PORT EXCITATION

The pattern when a single port is excited consists of the broad pattern of the element with a notch at the angle of the peak of the frequency-scanned array (except for the final elements). The details of the pattern depend on the coupling coefficient of the excited coupler, on the number of elements following, and on the distribution of coupling coefficients along the sinuous line. Since the 61-element array we have considered is representative of a number of frequency-scanned systems, its patterns for single-port excitation might be of interest in other applications (as for example Ajioka's use* of two such patterns, one deeply notched, the other not, to determine whether or not an interfering signal was in the main beam of the frequency-scanned array). A cosine element pattern was assumed, the distribution of coupling coefficients shown in Fig. 3 was used, and the pattern was calculated at a wavelength of 1.01, where the frequency-scanned beam was at -7 degrees. Figure D1 shows the patterns when various ports were excited.

*J.S. Ajioka, "Integral Auxiliary Antennas Derived from Arrays of Directionally Coupled Elements," invention disclosure, Feb. 1962, unpublished.

NRL REPORT 8226

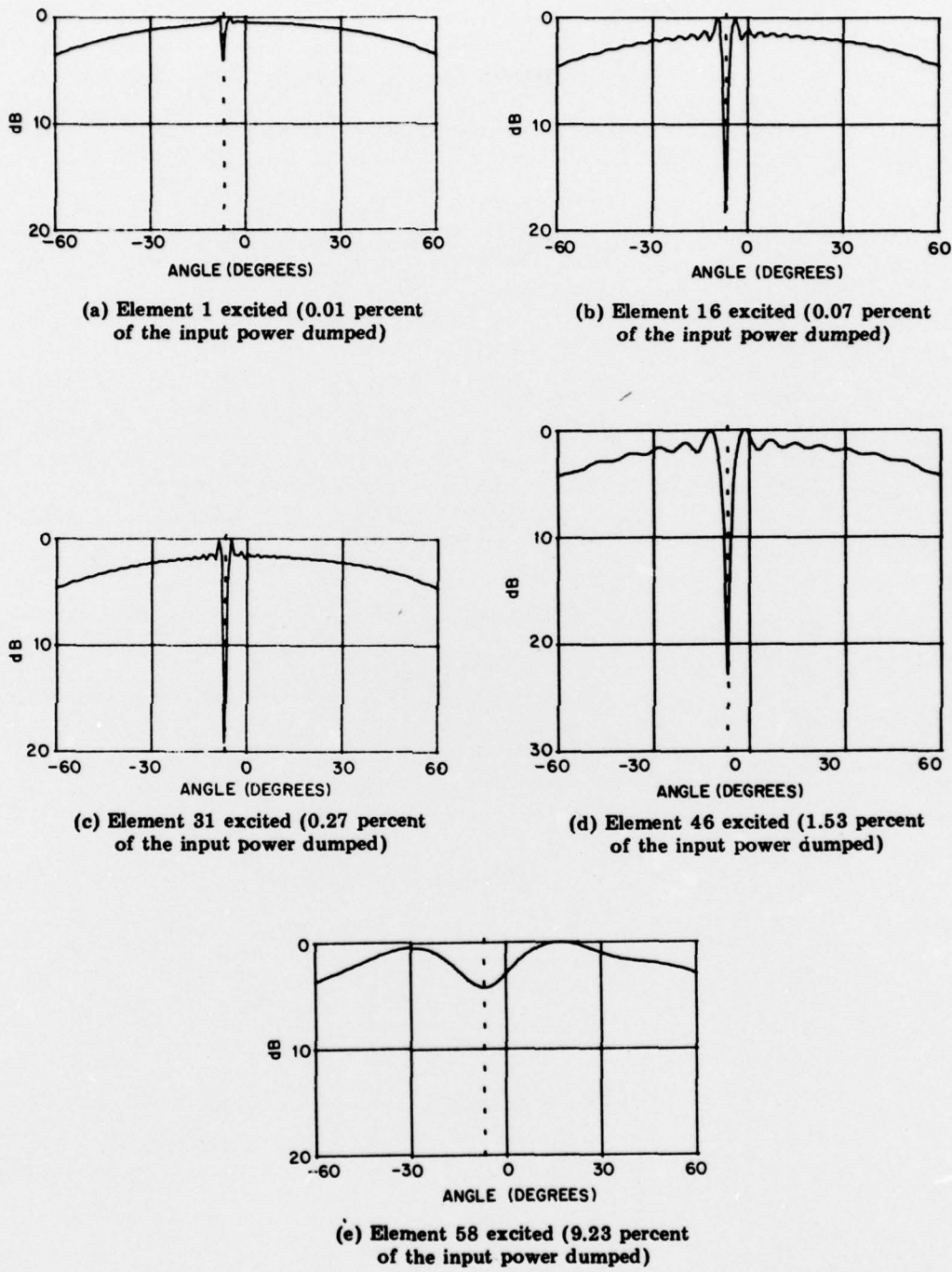


Fig. D1—Pattern when one element of the 61-element frequency-scanned array is excited, with $\lambda = 1.01$